Xavier Helan Flora, Mani Ulaganathan*, Karuppiah Kesavan, and Somasundaram Rajendran*

Synthesis of Bendable Plasticized Nanocomposite Polymer Electrolyte Using Poly(Acrylonitrile)/Poly (Methyl Methacrylate) Polymer Blends

Abstract: A class of nanocomposite polymer electrolytes (NCPE) with high ionic conductivity was prepared by blending of poly(acrylonitrile) and poly(methyl methacrylate) polymers. Lithium bis(trifluoromethanesulfonimide) ($LiN(CF_3SO_2)_2$), Ethylene carbonate (EC), Barium titanate ($BaTiO_3$) was used as ionic salt, plasticizers and ceramic filler, respectively. Role of inorganic ceramic filler on structural and ionic conductivity of the polymer electrolyte was investigated for various concentration**s** of $BaTiO_3$ filler. The structural elucidation, complex formation of the prepared electrolytes is ascertained from XRD, FTIR analysis. All the samples were subjected to complex ac impedance analysis for obtaining the bulk resistance of the composite electrolytes. It was found that the sample containing 10 wt. % of filler showed maximum ionic conductivity than the other samples. Thermal stability and surface morphology of the composite polymer electrolytes were also examined by thermogravimetric analysis and scanning electron microscope, respectively.

Keywords: Ceramic-Matrix Composites, Polymer-Matrix Composites (PMCs), X-Ray Diffraction (XRD), Scanning Electron Microscopy (SEM), Casting.

***Corresponding Author: Mani Ulaganathan,** Energy Research Institute@NTU(ERI@NTU), Nanyang Technological University, Singapore- 637 553, e-mail: nathanphysics@gmail.com
Somasundaram Rajendran, School of Physics, Alagappa University, Karaikudi-630 003, Tamil Nadu, India, e-mail: sraj54@yahoo.com
Xavier Helan Flora, Karuppiah Kesavan: School of Physics, Alagappa University, Karaikudi-630 003, Tamil Nadu, India
Xavier Helan Flora: Dept.of Physics, Kamaraj College, Tuticorin, Tamil Nadu, India

1 Introduction

Over the past four decades, there has been intensive research works carried out on polymer electrolytes in order to improve the specific energy and energy den-

sity of rechargeable Li-ion batteries. Earlier, P. V. Wright et al. studied the performance of the PEO based polymer-salt complex. Further works on the polymer electrolyte materials were mostly devoted to enhancing the ion transport properties. In spite of that, the polymer electrolyte is showing a poor room temperature ionic conductivity as a result still there has been a search for a polymer electrolyte with high ionic conductivity. So far various kinds of polymer electrolytes have been studied, among them, gel polymer electrolytes (GPEs) showed high ambient temperature ionic conductivity of the order of 10^{-3} S cm^{-1} which was composed of high dielectric plasticizers/solvents or their solution with different salts of lithium, sodium, *etc*. immobilized with a different polymer host such as poly(methyl methacrylate) (PMMA) [1], poly(vinylidene fluoride) (PVdF) [2], poly(ethylene oxide) (PEO) [3], poly(vinyl chloride) PVC [4] and poly(acrylonitrile) PAN [5]. The enhancement in ionic conductivity in plasticized electrolytes is explained in terms of ion association/dissociation effect and increase in the amorphous nature of the system [6]. Apart from various attractive properties, gel polymer electrolytes suffered from the poor mechanical properties. The conductivity and mechanical stability of GPEs are mutually exclusive, *i. e*., the ionic conductivity in GPEs increases at the expense of reduced mechanical strength, and vice versa [7]. One of the most recent approaches to circumvent the problem of electrolyte properties is the composite polymer electrolytes (CPE) which uses ceramic fillers (*e. g*., Al_2O_3, TiO_2, SiO_2, $BaTiO_3$, *etc*.) as additive [8–10]. The properties of these composites have been determined by the individual phases, morphology, size of the dispersed phase, distribution and orientation of the ceramic fillers [11]. Croce et al [12]. have developed models to explain the enhanced ionic transport properties in polymer inorganic composite electrolytes in which acid, normal and basic surface-functional groups are attached on nano-sized fillers. Magistris and co-workers [13, 14] reported that the addition of inorganic ceramics (such as Al_2O_3, SiO_2, *etc*.) into the polymer electrolyte had been shown to improve the mechanical property, the working temperature of the electrolytes and the stability of the electrode–electrolyte interface. Ragavan et al [15]. reported that $BaTiO_3$ incorporated P(VdF-co-HFP) based membrane exhibited better mechanical property than the membrane with other fillers Al_2O_3, SiO_2 *etc*. Even though a number of nanocomposite polymer electrolytes studied over the years, combining high ionic conductivity along with a good mechanical and electrochemical stability of the polymer electrolytes still remains a challenge to the lithium ion battery technology.

In the present work, ferroelectric $BaTiO_3$ has been used as ceramic filler; $BaTiO_3$ has widespread applications as a capacitor material because of its high dielectric constant (10^3 to 10^5). Ferroelectric domain as well as high dielectric nature of $BaTiO_3$ facilitates salt dissociation into charged species and produces a higher

volume of the amorphous phase; as a result, the conductivity of the polymer electrolyte can be enhanced further [16]. In the present scope, an attempt is made on the preparation of polymer blend electrolytes using PAN and PMMA polymers complexed with $LiN(CF_3SO_2)_2$ for various concentration of $BaTiO_3$ filler and the effect of concentration of the $BaTiO_3$ filler on the ionic conductivity and structural changes are investigated.

2 Experimental

2.1 Sample preparation

PAN (*avg. Mw* 94 000) and PMMA (*avg. Mw* 120 000) were purchased from Aldrich chemicals ltd, USA. The polymers were dried at 110 °C under vacuum for 10 h; the lithium salt $LiClO_4$ (Aldrich) was dried at 70 °C under vacuum for 10 h; Ethylene carbonate (EC) was used as received. $BaTiO_3$ procured from Aldrich, USA of particle size 55 nm was used after annealing at 373 K for 12 h.

All the nano composite polymer electrolytes were prepared using solvent casting technique. Appropriate amount of PAN, PMMA and $LiClO_4$ were dissolved by addition, in sequence, to Di-methyl formamide (DMF) (E. Merck, Germany). After incorporating the given amount of plasticizer EC, inorganic filler $BaTiO_3$ was suspended in the solution and stirred continuously at room temperature. Thus the obtained composite slurry was cast by spreading the suspension onto a finely polished Teflon bushes and Teflon covered glass plates. The films were dried in a vacuum oven at 333 K under a pressure of 10^{-3} Torr for 24 h to remove further traces of solvent. The resulting films were visually examined for their dryness and free-standing nature.

2.2 Characterization techniques

XRD patterns have been obtained using X'Pert pro PANalytical diffractometer using Cu-Kα radiation having a wavelength of 1.5417 Å. The sample was scanned in the 2θ ranging from 10–80° for 2 sec in the step scan mode. FTIR spectroscopy has been performed using (Perkin–Elmer) spectrophotometer in the wavenumber range 400–4000 cm^{-1}. Ac impedance measurement was performed using Keithley LCZ meter (model 3330). The electrolyte samples were sandwiched between the two stainless disc electrodes of the sample holder and connected to LCZ meter. The data acquisition has been carried out in the frequency range from 40 Hz to 100 kHz and in the temperature range from 303 to 373 K. The thermal stabil-

Table 1: Temperature dependent ionic conductivity values.

Sample Code	PAN (18 wt. %) – PMMA (6 wt. %) $LiN(CF_3SO_2)_2$ (8 wt. %)/EC (68 wt. %) $BaTiO_3$ (X wt.%)	Temperature dependent conductivity values $\times 10^{-3}$ S cm^{-1}				
		303 K	318 K	333 K	353 K	373 K
F1	$X = 0$	0.263	1.520	4.270	10.70	14.80
F2	$X = 5$	1.320	3.550	7.410	15.50	19.50
F3	$X = 10$	9.120	20.90	36.30	59.00	63.10
F4	$X = 15$	4.900	12.60	22.90	36.40	43.70
F5	$X = 20$	2.820	6.760	14.10	25.70	31.00

ity of the electrolytes were studied from ambient to 400 °C temperature range by thermo gravimetric analysis (TGA) Perkin Elmer (pyres diamond, USA)) at a heating rate of 10 °C min^{-1} under nitrogen atmosphere. The surface morphology of the samples was examined using a JEOL JSM-840A scanning electron microscope (SEM).

3 Results and discussion

3.1 XRD Analysis

X-ray diffraction pattern provides the structural information of the prepared samples. Figure 1 shows the XRD patterns of $LiN(CF_3SO_2)_2$, $BaTiO_3$, PAN, PMMA, and composite polymer electrolyte membranes (F1–F5). The XRD pattern of pristine PAN shows a sharp crystalline peak around at 2θ =16.43° and a broad hump around 28–29°. The characteristic peak obtained at 16.43° corresponds to (110) reflection confirms orthorhombic structure of the PAN polymer [17]. The broad diffraction peak of PMMA reveals its complete amorphous nature. The characteristic peaks at $2\theta = 22$, 31, 45, 51, 56, 65, 70 and 75° confirm the high crystalline nature of $BaTiO_3$ inorganic filler. The particle size of the filler is calculated for each θ value individually using Debye–Scherrer formula ($D = 1.94\lambda/\beta \cos\theta$) and the calculated average particle size is 55 nm. XRD pattern of $LiN(CF_3SO_2)_2$ shows high intensity diffraction peaks confirming the complete crystalline nature of the lithium salt. It is noted that the ionic conductivity is increased with the decrease of crystallinity of the complex matrix due to the fact that ionic conduction essentially occurs through the amorphous phase in the polymer electrolytes [9]. A higher degree of amorphous phase has been observed for the complex F3; hence the conductiv-

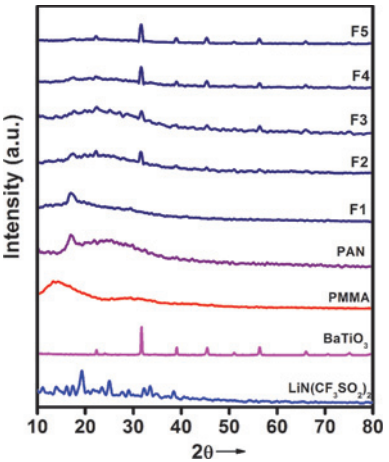

Figure 1: X-ray diffraction analysis spectra of the pure and prepared samples.

ity is higher for that composite electrolyte film. It is also observed that the intensity of the peak gets increased for the samples which holds filler content above the optimum level (10 wt. %); as a result the fillers in-situ in the complexes builds more immobile blocks like aggregation or agglomeration in the matrix which could be the reason for lower conductivity observed in the composite films F4 & F5. Presence of aggregation of the filler in the nanocomposites was also confirmed from the SEM images. This result is in close agreement with the earlier reports based on the PVAc-PVdF-co-HFP-$BaTiO_3$ [18, 19] and TiO_2 incorporated PMMA/PEGDA blend composite electrolyte system [20].

3.2 FTIR analysis

In order to investigate the complex formation and interactions between the various constituents in the polymer electrolyte complexes, FTIR studies have been carried out [21] (Figure 2). The vibrational frequencies appeared at 2939, 1632, 1246 are assigned to CH_2 asymmetrical stretching, CH asymmetrical stretching, inplane symmetrical C-N stretching frequencies of pristine PAN respectively. The vibrational band at 2249 cm^{-1} corresponds to the stretching vibration of nitrile band (C≡N) of PAN which is shifted towards the lower frequency side in all the complexes. This is due to the inductive effect created by the interaction between the nitrogen atoms in C≡N with Li^+ ion [22]. In PMMA, the C=O symmetrical stretch, $-O-CH_3$ stretching vibrations, $-CH_3$ symmetrical bending, $-CH_2$ wagging, C–O–C

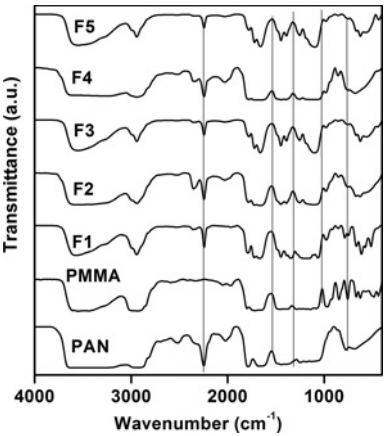

Figure 2: FTIR analysis spectra of the pure and prepared samples.

bending and $-CH_2$ rocking modes give sharp peaks at 1735, 1450, 1383, 981, 842 and 754 cm^{-1}, respectively. The peaks at 1788, 1782, 1779,1780 and 1779 cm^{-1} in the complexes F1, F2, F3, F4 and F5 respectively correspond to the $\nu_{C=0}$ (1788 cm^{-1}) band of Ethylene carbonate. The vibrational peak at 1493 cm^{-1} of pure EC is shifted to 1486, 1486, 1487, 1490, 1483 in the complexes.

The vibrational absorption peak corresponds to $\nu_{asym}(SO_2)$-in-plane stretching vibration of SO_2 of imide anion is obtained at 1355 cm^{-1} [23] and is shifted to 1347 cm^{-1} in the complex F1. For pristine imide salt, the S-N-S symmetrical stretching vibrational band obtained at 798 cm^{-1} [24] is also shifted to the lower wave number side in the complexes. The asymmetric in plane bending mode of SO_2 of the anion is obtained at 618 cm^{-1} and asymmetric bending vibration of CF_3 at 575 cm^{-1} in solid imide shift to a slightly lower wave number side in the nano composites.

Apart from these, some new peaks are found and few vibration peaks corresponding to the pristine materials are absent in the complex systems. Thus the spectral analysis confirms the complexation among the constituents of the polymer matrices.

3.3 Conductivity studies

Figure 3 represents the Nyquist plot of PAN/PMMA/EC/$LiN(CF_3SO_2)_2$/$BaTiO_3$ (10%) at room temperature. It can be seen that the imaginary part of the impedance is linearly related to its real part. The intersection of the straight line

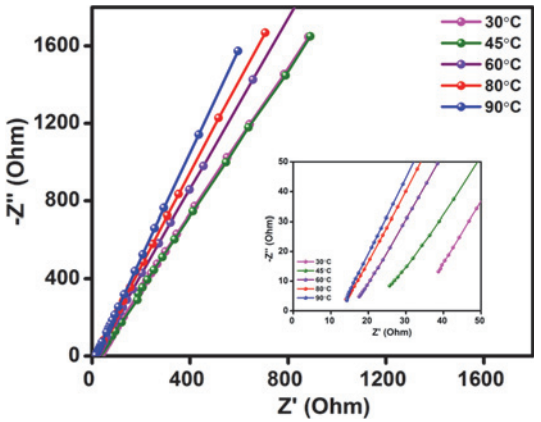

Figure 3: Ac impedance analysis spectra of the sample exibiting maximum ionic conductivity.

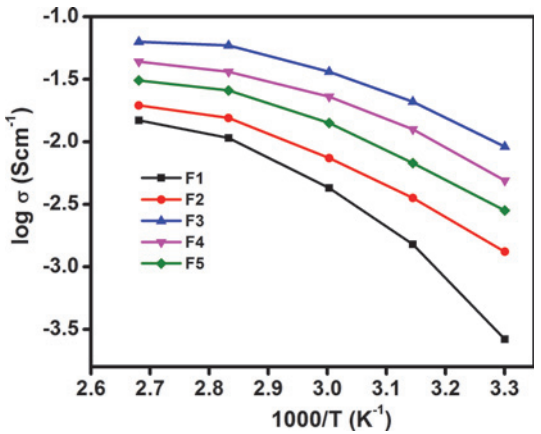

Figure 4: Teperature dependant ionic conductivity plot of the prepared composite polymer electrolytes.

with the real axis gives the bulk resistance (R_b) of the electrolyte. Ionic conductivity of the CPE is calculated using $\sigma = l/R_b A$, in which l is the thickness of NCPE, and A is the active area of the samples.

Figure 4 shows the relationship between $\log \sigma$ vs. $1000/T$ of the prepared NCPEs. Typical behaviour of the increase of conduct ivity with the temperature of the lithium polymer electrolytes has been confirmed for the NCPEs (Table 1). It is a well known fact that the external thermal energy to the polymers can encourage the segmental motion of the polymer chains which results in an increase in free volume of the electrolyte. Thus the segmental motion either permits the

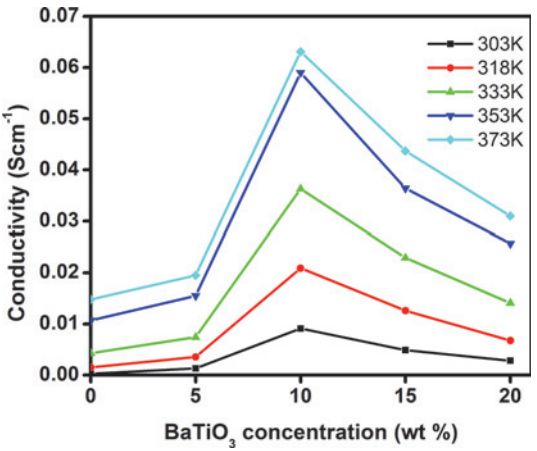

Figure 5: Effect of filler concentrations on PAN: PMMA (75/25) wt. %) $LiN(CF_3SO_2)_2$ (8 wt. %) EC (68 wt. %) $BaTiO_3$ (X) $(X = 0, 5, 10, 15, 20)$ complexes at different temperatures.

ions to hop from one site to another site or provides an easy pathway for the transitional motion of the ions. This leads to an increase in ion mobility and segmental mobility that will assist ion transport and virtually compensate for the retarding effect of the ion clouds in the electrolyte. The ionic conductivity of the composite gel polymer electrolyte increases with the increase of temperature but it is not related to the temperature in a linear relationship. This suggests that the conductivity of the electrolyte can be best described by the Vogel–Tamman–Fulcher (VTF) relation, which is the characteristic of the amorphous polymeric electrolytes [25].

The temperature dependence of polymer electrolyte membrane as a function of filler content is shown in Figure 5. The ionic conductivity increases with the increase in filler content and the maximum ionic conductivity is obtained for 10 wt. % of $BaTiO_3$ incorporated system (Table 1). Further increase of the filler content in the plasticized complex has decreased the conductivity because of the aggregation of the fillers [26]. As commonly found in composite materials, the conductivity is not a linear function of the filler concentration. The composite conductivity has been found to be dependent on several parameters viz. surface acidity of oxides, volume fraction and particle size, solvent dielectric constant, salt concentration and temperature. The increase of conductivity is probably due to the following reason. Firstly, Ferroelectric fillers such as $BaTiO_3$ are expected to decrease the interfacial resistance between the lithium anode and the polymer electrolyte due to the permanent dipole of the ferroelectric materials. In composite polymer electrolytes, the permanent dipole of the ferroelectric could act as an

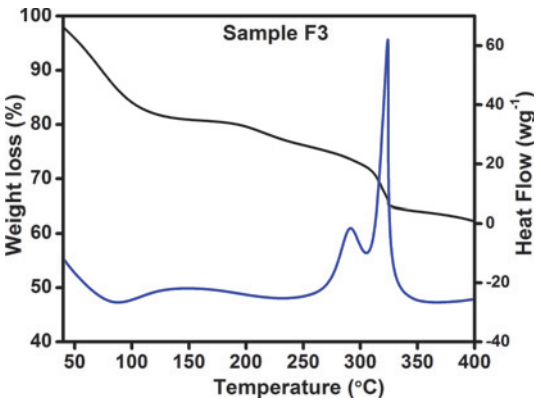

Figure 6: TG/DTA thermogram of PAN (18 wt. %) – PMMA (6 wt. %) $LiN(CF_3SO_2)_2$ (8 wt. %) EC (68 wt. %) $BaTiO_3$(10%).

origin of the Lewis acid base interaction and form a highly conductive layer at the electrolyte/filler interface by strong interaction with the other constituents in the polymer electrolytes, showing higher ionic conductivity than the pristine polymer electrolyte [27]. Secondly, the addition of the filler with reduced particle size tends to contribute uniformly to the reduction in crystallinity of the polymer matrix by promoting effectively the dissociation of ion-ion pairs and ion clusters in the polymer electrolytes with the help of the strong electrostatic interaction caused by permanent dipoles. The overall effect of the plasticizer and the filler, would lead to a considerable conductivity enhancement in the filler-added, plasticized polymer electrolyte system. But at higher filler contents, continuous non-conductive phase built up by large amount of fillers as an electrically inert component would block up lithium ion transport, resulting in increase in the total resistance of the composite polymer electrolyte. It is concluded from the study that the conductivity of the studied composite polymer electrolyte is appreciable and hence NCPE is suitable for the fabrication of possible electrochemical devices.

4 TG analysis

The thermal stability of the composite electrolyte has been estimated in terms of the degradation temperature values observed from the TGA data. Thermogram of the sample exhibiting maximum ionic conductivity is depicted in Figure 6. TG curve of the sample reveals that the sample starts to lose its weight around at 100 °C. This initial loss is due to the evaporation of residual solvent or by the ab-

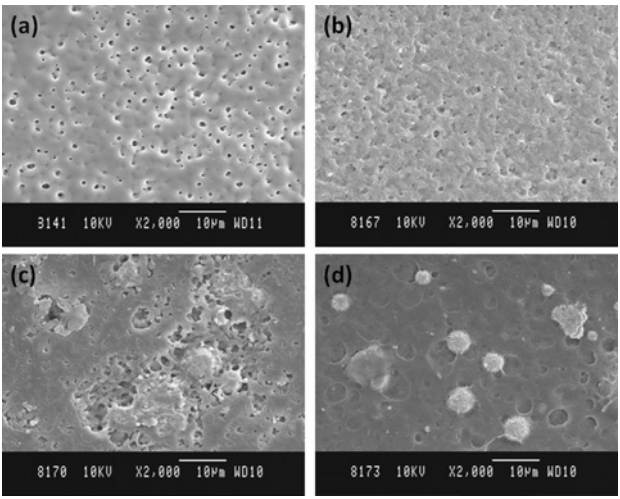

Figure 7: SEM images of the sample F1, F3, F4 and F5.

sorption of moisture during the loading of the sample for TGA analysis. A second decomposition takes place at 310 °C accompanied by a weight loss of 23 wt. %, this may be due the decomposition of the polymers used in the electrolyte preparation since most of the organic polymers can degrade in the temperature range of 200–300 °C. The obtained thermogram of the sample indicates that the film is stable upto 310 °C. The improved thermal stability of the electrolytes compared with pristine polymer electrolyte is attributed to the addition of $BaTiO_3$ content in the system. The above weight losses of the sample are also confirmed from the endothermic peaks of the DTA curves.

5 Scanning electron microscopic studies

SEM images of the samples without and with the addition of $BaTiO_3$ filler are shown in Figure 7. It is a well known fact that the porosity of the polymer electrolyte is one of the important parameters of porous polymer membranes in lithium batteries [28, 29]. Presence of pores in microstructure is due to solvent evaporation, since the blended polymer electrolyte has higher solvent retention ability. It is observed from film (F3) that the membrane has large number of pores of small size compared with membrane containing 0% $BaTiO_3$. The porous structure of the membrane leads to the entrapment of large volume of the liquid in the

cavities, which forms a connected path through the polymer matrix [30], accounting for the increased ionic conductivity. Saito et al. [31], reported that the porosity dominate the conduction properties of the carriers in some GPEs. At high concentration of filler (F4 and F5), aggregation of nanocomposite particles is confirmed which tends to restrict the ionic movement. This result is in close agreement with the conductivity studies.

6 Conclusions

It is found that the incorporation of barium titanate into the PAN-PMMA-$LiN(CF_3SO_2)_2$ electrolyte enhances the ionic conductivity of the complex. The maximum room temperature ionic conductivity is obtained for 10 wt. % of $BaTiO_3$ added PAN-PMMA-$LiN(CF_3SO_2)_2$ sample and the value is about $9.12 \cdot 10^{-3}$ S cm^{-1}. However, the ionic conductivity of the complex has decreased above 10 wt. % of filler which is due to the building of aggregation of the nanoparticles in the complex. Temperature dependent conductivities of the samples are discussed on the basis of free volume model. It is noted that the sample exhibiting maximum conductivity is also stable upto 310 °C. Hence, it is concluded that the prepared nanocomposite polymer electrolytes are more suitable for the possible device fabrications.

Received December 2, 2013; accepted February 25, 2014.

References

1. J.-D. Jeon, B.-W. Cho, and S.-Y. Kwak, J. Power Sources **143** (2005) 219.
2. Z. H. Li, P. Zhang, H. P. Zhang, Y. P. Wu, and X. D. Zhou., Electrochem. Comm. **10** (2008) 791.
3. H. Cheng, C. Zhu, B. Huang, M. Lu, and Y. Yang, Electrochim. Acta **52** (2007) 5789.
4. T. Janaki Rami Reddy, V. B. S. Achari, A. K. Sharma, and V. V. R. Narasimha Rao, Ionics **13** (2007) 55.
5. F. Yuan, H.-Z. Chen, H.-Y. Yang, H.-Y. Li, and M. Wang, Mater. Chem. Phys. **89** (2005) 390.
6. D. K. Pradhan, B. K. Samantaray, R. N. P. Choudhary, and A. K. Thakur, J. Power Sources **139** (2005) 384.
7. S. Ahmad, H. B. Bohidar, S. Ahmad, and S. A. Agnihotry, Polymer **47** (2006) 3583.
8. H.-W. Chen and F.-C. Chang, Polymer **42** (20012) 9763.
9. S. Panero, D. Satolli, A. D. Epifano, and B. Scrosati, J. Electrochem. Soc. **149** (2002) A414.
10. S. Kim and S.-J. Park, Solid State Ionics **178** (2007) 973.

11. S.-J. Park and B.-R. Jun, J. Colloid Interf. Sci. **284** (2005) 204.
12. F. Croce, L. Persi, B. Scrosati, F. Serraino-Fiory, E. Plichta, and M. A. Hendrickson, Electrochim. Acta **46** (2001) 2457.
13. C. Capiglia, P. Mustarelli, E. Quartarone, C. Tomasi, and A. Magistris, Solid State Ionics **118** (1999) 73.
14. E. Quartarone, P. Mustarelli, and A. Magistris, Solid State Ionics **110** (1998) 1.
15. P. Raghavan, X. Zhao, J.-K. Kim, J. Manuel, G. S. Chauhan, J.-H. Ahn, and C. Nah, Electrochim. Acta. **54** (2008) 228.
16. H. Y. Sun, H.-J.Sohn, O. Yamamoto, Y. Takeda, and N. Imanishi, J. Electrochem. Soc. **146** (1999) 1672.
17. D. Sawai, M. Miyamoto, T. Kanamoto, and M. Ito, J. Polym. Sci: Polym. Phys. **38** (2000) 2571.
18. M. Ulaganathan, R. Nithya, S. Rajendran, and S. Raghu, Solid State Ionics **218** (2012) 7.
19. S. Rajendran, K. Kesavan, R. Nithya, and M. Ulaganathan, Curr. Appl. Phys. **12** (2012) 789.
20. H.-S. Kim, K.-S. Kum, W.-I. Cho, B.-W. Cho, and H.-W. Rhee, J. Power Sources **124** (2003) 221.
21. R. John, *Applications of Absorption Spectroscopy of Organic Compounds*, Dyer, Prentice Hall of Pvt. Ltd., New Delhi, 1991.
22. Z. Osman, K. Bahiyah Md Isa, and A. Ahmad, Ionics **16** (2010) 431.
23. I. Rey, P. Johansson, J. Lindgren, J. C. Lassegues, J. Grondin, and L. Servant, J. Phys. Chem. A **102** (1998) 3249.
24. A. Bakker, S. Gejji, J. Lindgren, K. Hermansson, and M. M. Probst, Polymer **36** (1995) 4371.
25. J. P. Sharma and S. S. Sekhon, Solid State Ionics **178** (2007) 439.
26. T. Itoh, Y. Ichikawa, T. Uno, M. Kubo, and O. Yamamoto, Solid State Ionics **156** (2003) 393.
27. Z. Wen, T. Itoh, T. Uno, M. Kubo, and O. Yamamoto, Solid State Ionics **160** (2003) 141.
28. Q. Shi, M. Yu, X. Zhou, Y. Yan, and C. Wan, J. Power Sources **103** (2002) 286.
29. J. Saunier, F. Alloin, J. Y. Sanchez, and G. Caillon, J. Power Sources **119–121** (2003) 454.
30. Y.-J. Hwang, K. S. Nahm, T. Prem Kumar, and A. M. Stephan, J. Membr. Sci. **310** (2008) 349.
31. Y. Saito, A. M. Stephan, and H. Kataoka, Solid State Ionics **160** (2003) 149.